

Studies on Composite PVA-CA-NH₄CF₃SO₃-Al₂O₃ Polymer Electrolyte for Electrochemical Devices

S. GURULAKSHMI^{1,2,10}, S. MADESWARAN^{1,*10}, S. KARTHIKEYAN^{3,10} and V. PORCHEZHIAN⁴

¹School of Advanced Sciences, VIT University, Vellore-600127, India

²Department of Physics, Guru Nanak College, Chennai-600042, India

³Department of Physics, Madras Christian College, Chennai-600059, India

⁴Department of Chemistry, Guru Nanak College, Chennai-600042, India

*Corresponding author: E-mail: madeswarans@gmail.com

Received: 7 January 2019;

Accepted: 19 February 2019;

Published online: 28 March 2019;

AJC-19352

In the present study, polymer electrolyte with poly(vinyl alcohol) (PVA) blended with cellulose acetate (CA) was chosen to prepare composite electrolyte using ammonium triflate salt and nano sized alumina (Al₂O₃ < 50 nm) by the solution casting method. The as prepared samples were characterized by X-ray diffraction, FT-IR, differential scanning calorimetry and AC impedance spectra. The loss tangent and dielectric studies were carried out for all the prepared samples using AC impedance analysis. Activation energy with regression values and relaxation time were calculated and found to be low for the highest conducting membranes. The presence of 0.1 mol content of nano alumina has enhanced the ionic conductivity significantly to the value of 2.012×10^{-3} S/cm from that of the filler-free electrolyte (2.93×10^{-4} S/cm). Ionic transference number was calculated by electrostatic polarization method and it was found to be 0.9684, which shows the conducting species were ions. A proton battery fabricated using the configuration Zn+ZnSO₄.H₂O || PVA-CA-0.5 mol NH₄CF₃SO₃-0.1 mol Al₂O₃ || PbO₂ + V₂O₅ produced a steady state open circuit voltage of 1.39 V, which proves the prepared composite electrolyte is suitable solid electrolyte for electrochemical devices.

Keywords: FT-IR, Ionic conductivity, Dielectric analysis, Poly(vinyl alcohol), Cellulose acetate, Ammonium triflate, Nano alumina.

INTRODUCTION

In the process of achieving a good solid electrolyte for electrochemical devices the composite polymer electrolytes plays an important role. Over the past few years, many polymer blends with different lithium and ammonium salts have been reported as a potential polymer electrolyte material for solid state batteries and other electrochemical devices [1-3]. In the preparation of proton exchange membrane materials, different polymers like SPEEK, PVdF, PMMA, PVA, cellulose acetate, PEO, PANI and nano wires were used [4,5]. Among those, poly(vinyl alcohol) has been widely used because of its potential property to form good miscible blends. Poly(vinyl alcohol) has been separately reported to produce highly conducting electrolytes with salts and acids [6], but its mechanical stability is always a concern for the application of those membranes as a potential electrolyte for solid state electrochemical devices. Further, the blending of natural polymers like cellulose acetate with poly(vinyl alcohol) has been shown to give notable incre-

ments in the conductivity values and its mechanical stability. However, the ionic conductivity value was not preferable for the application in electrochemical devices. This problem can be overcome by the incorporation of organic/inorganic nano fillers with suitable ammonium salt complex polymer electrolytes [7].

The usage of ammonium triflate salt has enhanced the ionic conductivity, as one of the H atoms in the NH₄⁺ ions of ammonium triflate is weakly bound to the polar group of host polymers and it easily dissociates under the electric field [8]. The transport of H⁺ ions by Grotthus mechanism through the coordinating sites of polymer matrix is the main reason for selecting this salt as a dopant in our system. From the earlier works reported by many researchers [9-11], the incorporation of inorganic fillers over the organic fillers reduces the cost of polymer electrolyte and thus the nano alumina was chosen to be a filler material. It helps to enhance H⁺ transport through the expected interaction between the surface group of fillers and the migrating ions.

Hence in the present study poly(vinyl alcohol) (PVA) and cellulose acetate (CA) were used as the base polymers for blend. Ammonium triflate was chosen as the dopant salt and nano-sized alumina was chosen as the inorganic filler in order to study the conductivity behaviour of composite polymer electrolytes. Their application on proton battery is also investigated using the maximum conducting composite membrane as an electrolyte.

EXPERIMENTAL

Poly(vinyl alcohol) (PVA, $M_w = 1,25,000$, 88 % hydrolyzed, AR grade, MERCK made) and cellulose acetate (CA, Loba made) were used as starting materials for polymer blending and ammonium trifluoro methane sulfonate (ammonium triflate-AT) ($\text{NH}_4\text{CF}_3\text{SO}_3$, Sigma-Aldrich) salt was used as the dopant in the polymer blend. Nano-sized alumina powder (average particle size of $\sim < 50\text{nm}$) (Sigma-Aldrich made) was used as the inorganic filler with dimethyl sulfoxide as a solvent. All the chemicals were used as procured from the manufacturer.

Preparation of composite electrolytes: The entire polymer electrolytes were prepared by conventional solution casting method. The ratio of PVA and cellulose acetate in this study was used as reported in our previous work [5]. The different mol contents of $\text{NH}_4\text{CF}_3\text{SO}_3$ (AT) salt with the optimized polymer blend were dissolved in DMSO and magnetically stirred to get the homogenous solution. Each mixture was stirred at 45°C for 24 h to achieve complete dissolution. The resulting solution was poured in the clean polypropylene petri dish and the solvent was evaporated using hot air oven. After optimizing the salt concentration for the best conducting electrolyte, the nano-sized alumina in different mol concentrations were added in the aforesaid mixture and the same procedure was used to get the composite polymer electrolyte membrane for the investigation. The prepared membranes were kept in a desiccator until use.

Characterization: X-ray diffraction patterns of the polymer electrolytes at room temperature have been obtained by Philips X-Ray diffractometer with CuK_α radiation in the 2θ range from 5° to 60° at a scan speed of $2^\circ/\text{min}$. FT-IR spectroscopy was used to study the interaction between salt and polymer in the electrolyte using SHIMADZU-8000 spectrophotometer in the range $4000\text{--}600\text{ cm}^{-1}$ with the scanning rate of 50 scans per second. Thermal analyses of polymer electrolytes were carried out by differential scanning calorimetry technique (DSC) (NETZSCH DSC-204) at a temperature range of $298\text{--}523\text{ K}$ in nitrogen atmosphere. AC impedance spectroscopy studies were done by broadband dielectric/impedance spectrometer – Novo control Technologies to measure the impedance with frequency limit up to 10 MHz. Moreover, dielectric and loss tangent studies were also conducted. The highest conductive membrane was chosen for the construction of proton battery.

RESULTS AND DISCUSSION

XRD studies: The XRD patterns for PVA-CA-AT- $x\text{ Al}_2\text{O}_3$ ($x = 0, 0.06, 0.08, 0.1$ and 0.3 mol) polymer composites are shown in Fig. 1. The crystalline nature of the polymer composites is correlated with the intensity of the diffraction peaks with reference to the work done by Hodge *et al.* [12]. Accord-

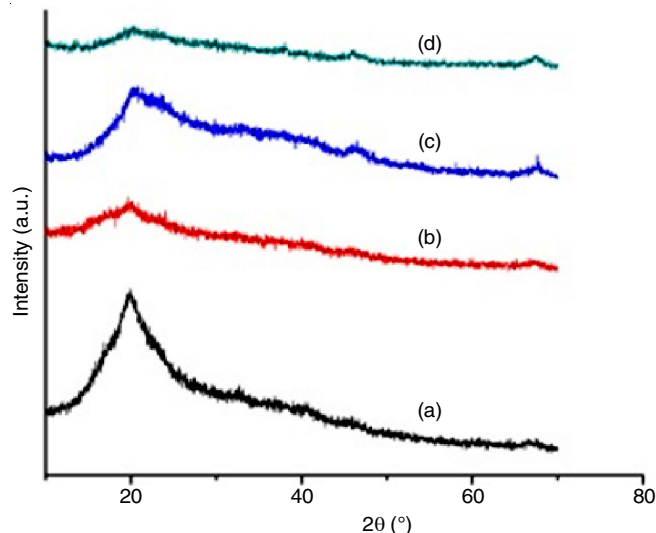


Fig. 1. XRD patterns for PVA-CA-AT- $x\text{ Al}_2\text{O}_3$ (a) $x = 0$, (b) 0.06, (c) 0.08 and (d) 0.1 mol polymer composites

ding to them, the reductions in intensity of the diffraction peaks are related to the amorphous nature of the polymer. The nano alumina free polymer electrolyte has relatively high intensity diffraction peaks (curve a) and it reduces with increase in the nano alumina concentration in polymer composites (curves b-d). The sample containing 0.1 mol Al_2O_3 shows less intensity of XRD peaks, which refers to the increase in amorphous nature of the polymer composite by the addition of nano alumina [9]. These results are comparable with the conductivity values of the polymer composites calculated by AC impedance spectroscopy analysis. With higher concentrations of alumina, small diffraction peaks in the region of $2\theta = 46^\circ$ and 67° are observed, which may be attributed to the presence of alumina in the polymer composite.

FT-IR studies: The FT-IR spectra obtained for pristine PVA, PVA-CA and for PVA-CA-AT- $x\text{ Al}_2\text{O}_3$ ($x = 0, 0.06, 0.08, 0.1$ and 0.3 mol) are shown in Fig. 2. This analysis was performed to confirm the blending between the two polymers and the interaction of salt and filler with the polymer matrix. From

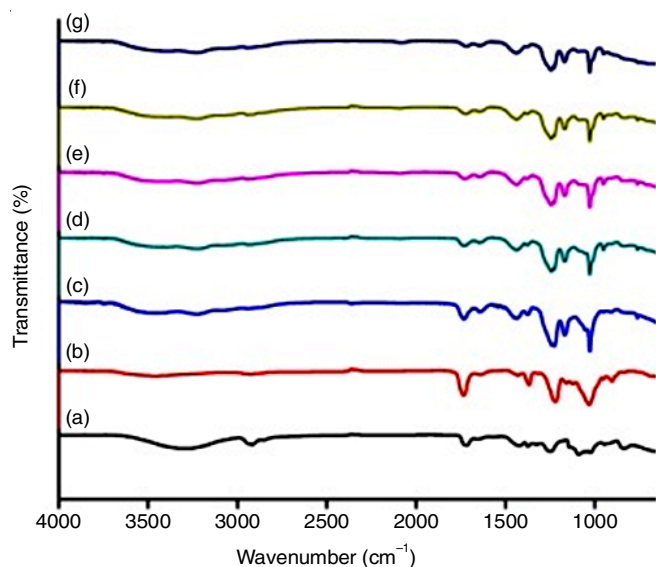


Fig. 2. FT-IR spectra for (a) pristine PVA, (b) PVA-CA and (c-g) PVA-CA-AT- $x\text{ Al}_2\text{O}_3$ ($x = 0, 0.06, 0.08, 0.1$ and 0.3 mol)

the spectrum of pristine PVA, a strong broad vibration band at 3291 cm⁻¹ is observed due to the intermolecular hydrogen bonding and the hydroxyl (O-H) stretching vibration of PVA. The peaks observed at 2940, 2916, 1088 and 1328 cm⁻¹ are attributed to the asymmetrical stretching of C-H bond, symmetrical stretching of C-H bond, stretching vibration of C-O and O-H bending of pure PVA [13] respectively. The peak responsible for O-H stretching in cellulose acetate is observed at 3466 cm⁻¹ in the PVA-CA blend spectrum. This confirms the complexation between the -OH groups of PVA-CA blend spectrum. The broad peak in this region indicates the significant number of -OH groups due to the unreacted -OH groups of PVA [11].

The wave number shifts in the region between 3470 and 3458 cm⁻¹ show that the hydroxyl bond shifted due to the addition of salt [14]. The peak observed in the PVA-CA spectra at 2920 cm⁻¹ is shifted to 2923 cm⁻¹ while adding the salt; this attributes to the symmetric C-H stretching [13]. The peak observed at 3225 cm⁻¹ in PVA-CA-AT- 0 mol Al₂O₃ spectra shows the asymmetric stretching of NH₄⁺ [15]. These results confirm the complexation between NH₄⁺ ion from ammonium triflate and -OH group of PVA-CA blend polymer [16]. The disappearance of the peak at 1317 cm⁻¹ from the PVA-CA spectra after the addition of salt confirms the breaking of -acyl group from the O-Ac functional group of cellulose acetate, allowing the oxygen as the unoccupied site for the transmission of cation from the salt [17]. From this interaction, the NH₄⁺ ion from ammonium triflate may be hydrogen bonded with the hydroxyl group of polymer or with the -O site of -O-Ac group of cellulose acetate.

The peaks observed at 761, 1027 and 1225 cm⁻¹ in PVA-CA-AT- x Al₂O₃ (x = 0, 0.06, 0.08, 0.1 and 0.3 mol) are referred to as δ_s(CF₃), ν_s(SO₃) and ν_s(CF₃) in free triflate ion, respectively. These results suggest that the free triflate ion is hydrogen bonded with the OH end groups [18]. The spectra for the nano-Al₂O₃ incorporated polymer complexes have observed no change in the vibrational bands and no new vibrational bands have been observed. This may be because the fillers are not chemically bound to the polymer matrix [19].

Differential scanning calorimetric analysis: DSC thermograms of pure PVA, PVA-CA and x mol Al₂O₃ with PVA-CA-AT- x Al₂O₃ (x = 0 and 0.1 mol) were shown in Fig. 3. As PVA is the semi crystalline polymer, it has both glass transition and melting temperature due to the presence of amorphous and crystalline phase. It is observed from (Fig. 3) the DSC thermogram (curve a) that the glass transition of 76 °C and the melting temperature of 189.7 °C for pure PVA electrolyte is close to the results reported by Agarwal & Awadhia [20] and Rudhzhia *et al.* [21]. The glass transition temperature for pure PVA is less than those reported earlier which may be due to the plasticization effect by the presence of DMSO solvent in the polymer electrolyte. The same may be the evidence for higher conductivity value (2.8 × 10⁻⁸ S/cm) obtained for pure PVA electrolyte membrane than the reported value (5.9 × 10⁻¹⁰ S/cm). The traces of DMSO in all composite electrolytes were evidenced by the small endothermic transition in the temperature range of 36-41 °C, which may be due to the interaction between DMSO and polymer matrix [20-22]. The same can be supported by the FT-IR results.

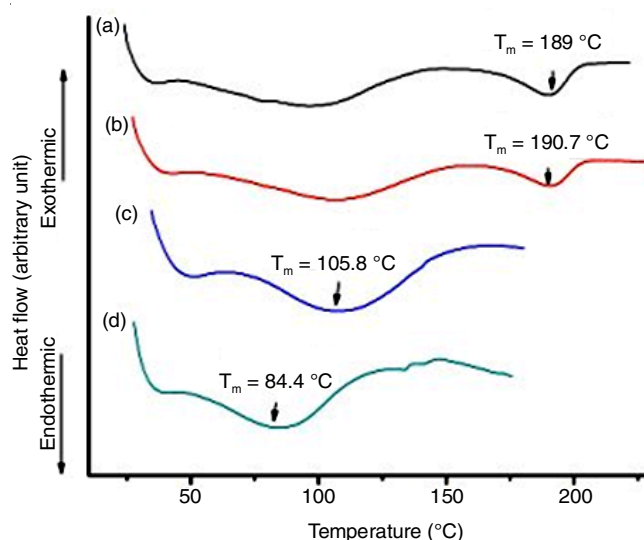


Fig. 3. DSC thermograms of (a) pure PVA, (b) PVA- CA and (c-d) x mol Al₂O₃ with PVA-CA-AT (x = 0 and 0.1 mol %)

The thermal behaviour of blended PVA-CA also resulted (curve b) in the same manner as that of pure PVA whose melting temperature is 190 °C. This may be due to the small amount of cellulose acetate present in the polymer matrix. But the heating enthalpy of pure PVA (33.94 J/g) is reduced by the blending of PVA-CA (24.39 J/g), which may refer to the increase in flexibility of polymer electrolyte.

Thermal behaviour of polymer is affected by the interaction of salt and fillers with that of the polymer matrix. The curves (c) and (d) indicate the thermal behaviour of polymer electrolytes of 0 mol Al₂O₃-PVA-CA-AT and 0.1 mol Al₂O₃-PVA-CA-AT, which shows the single broad endothermic transition at 106 °C (filler free) and 84.4 °C (with nano filler), respectively. The broad endothermic transition observed for the nano-filler free electrolyte (curve c) refers to the melting of PVA-CA-AT complex along with some uncomplexed PVA [23]. While observing the 0.1 mol Al₂O₃ added composite electrolyte, the broad endothermic transition is reduced to 84.4 °C. From this, it may be inferred that the melting temperature of the composite electrolyte has been reduced by the addition of nano-alumina fillers to the polymer matrix. These results well agree with the results reported by Agarwal, Masoud and Patel in their work [20,23,24]. This attributes that the addition of filler makes the composite polymer electrolyte more flexible and hence the reason for higher conductivity.

Impedance spectroscopy analysis: Fig. 4 shows the impedance plots (Z' vs. Z'') for the PVA-CA-AT-x mol Al₂O₃ (x = 0, 0.06, 0.08, 0.1 and 0.3 mol) composite polymer electrolytes at room temperature. It has a depressed semicircle with a long spike and the conductivity values are calculated by the relation given in eqn. 1:

$$\sigma = t/RA \quad (1)$$

where t is the thickness of the electrolyte membrane, R is the bulk resistance measured from the intercept of impedance plot and A is the area of the electrolyte. The conductivity values at room temperature for all the composite electrolytes are listed in Table-1.

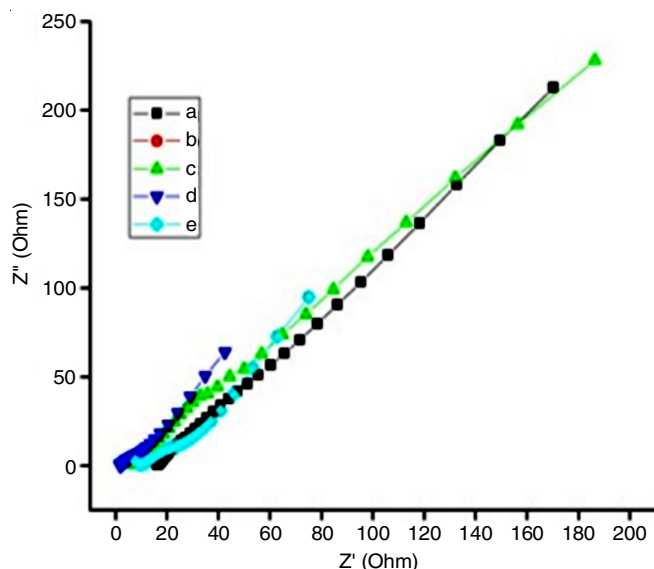


Fig. 4. Impedance plots (Z' vs. Z'') for PVA-CA-AT- x mol Al_2O_3 composite polymer electrolytes (a) $x = 0$ mol, (b) $x = 0.06$ mol, (c) $x = 0.08$ mol, (d) $x = 0.1$ mol, (e) $x = 0.3$ mol

TABLE-1
IONIC CONDUCTIVITY VALUES, ACTIVATION ENERGY AND RELAXATION TIME FOR PVA-CA-AT- x NANO- Al_2O_3 POLYMER MATRIX

x (mol)	Conductivity value (σ) (S/cm)	Activation energy (eV)	Regression value (R^2)	Relaxation time (s)
0	2.93×10^{-4}	0.165	0.9988	3.41×10^{-7}
0.06	3.04×10^{-4}	0.173	0.9999	4.46×10^{-7}
0.08	5.03×10^{-4}	0.197	0.9975	2.30×10^{-7}
0.10	20.12×10^{-4}	0.095	0.9806	2.24×10^{-7}
0.30	9.38×10^{-4}	0.197	0.9779	5.27×10^{-7}

Fig. 5 shows that the impedance plots for 0.1 mol Al_2O_3 content of composite electrolyte (which results in maximum conductivity) at different temperatures showed a similar behaviour.

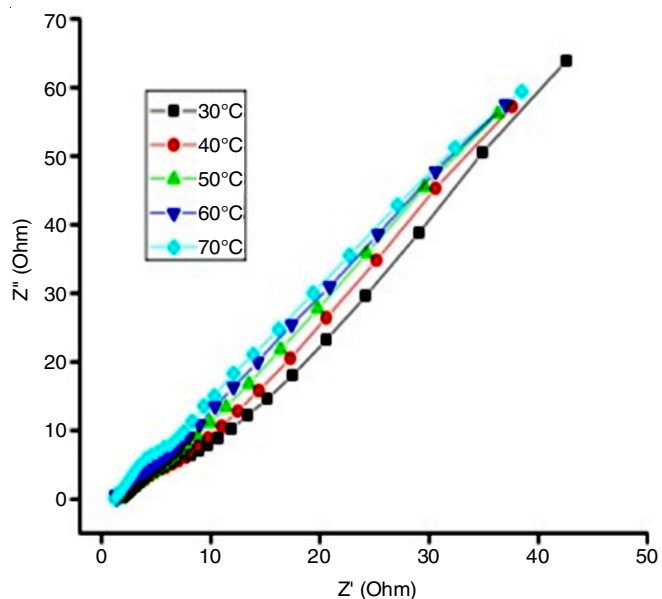


Fig. 5. Impedance plots (Z' vs. Z'') for 0.1 mol Al_2O_3 content of composite electrolyte at (a) 30 °C, (b) 40 °C, (c) 50 °C, (d) 60 °C, (e) 70 °C

Fig. 6 depicts the relationship of conductivity values with increasing Al_2O_3 concentration in the polymer matrix. This shows that the maximum conductivity value (2.12×10^{-3} S/cm) is observed for the 0.1 mol nano-alumina content, which can attribute to the point that addition of nano-alumina in the polymer matrix could increase the ion motion due to the increase in amorphous nature of this sample. The same sample has been shown to express high amorphous nature from XRD analysis. However, the conductivity value decreases with further increase in Al_2O_3 content, which can suggest that more aggregation of nano particles in the polymer matrix may block the path way of ions [19].

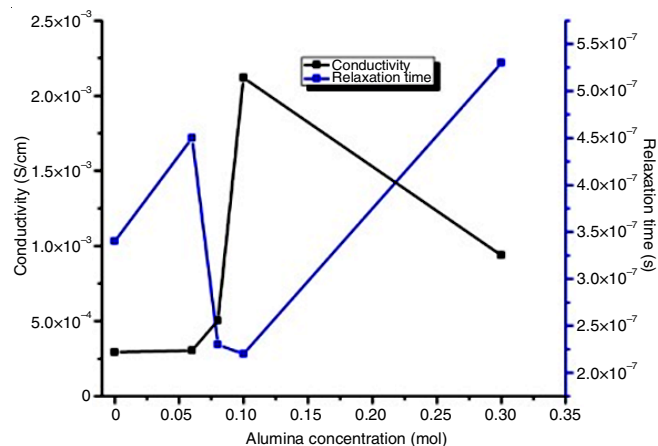


Fig. 6. Conductivity values and relaxation time with increasing Al_2O_3 concentration in polymer matrix

Fig. 7 shows the logarithm of conductivity with the reciprocal of absolute temperature for PVA-CA-AT- x Al_2O_3 ($x = 0, 0.06, 0.08, 0.1$ and 0.3 mol) composite polymer electrolytes and the plots are not completely linear as predicted by Arrhenius equation. Usually, the polymer electrolyte exhibits one of the five behaviours [25,26], thus our system exhibits Arrhenius behaviour at low temperature and VTF behaviour at high temperature and our results are comparable with those obtained by Huang *et al.* [25].

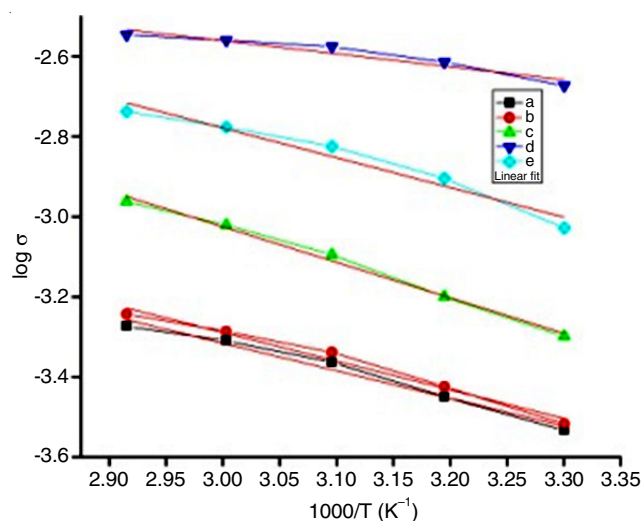


Fig. 7. $\log \sigma$ with the reciprocal of absolute temperature for PVA-CA-AT- x nano- Al_2O_3 composite polymer electrolytes (a) $x = 0$, (b) 0.06, (c) 0.08, (d) 0.1 and (e) 0.3 mol in the temperature region of 30-70 °C

The enhancement of conductivity values with increasing temperature for all the nano-Al₂O₃ added composite electrolytes can be attributed to the increase in flexibility in the polymer chain due to the decrease in their viscosity and Lewis acid-base type of interaction between the migrating ions and the O/OH groups on the Al₂O₃ surface; thus adsorption of anions on to the surface of Al₂O₃ reduces ion pairing, creating additional hopping sites for ionic motion [7]. The activation energies for transport of the conducting species are calculated from the linear plot of $\log \sigma$ versus $1000/T$ using Arrhenius equation in the temperature region 303-323 K as shown in Fig. 8. The calculated values are listed with the regression values in Table-1 and R² values are 0.99 and 0.98. This shows that the plots are linear fit and Arrhenius behaviour can be adopted for all the samples. From the table, the activation energy for the maximum conducting electrolyte with 0.1 mol Al₂O₃ content is observed to be low (0.095 eV) when compared with the Al₂O₃ free electrolyte (0.165 eV). The low value of activation energy can be attributed to the amorphous nature of the polymer composite, which facilitates H⁺ ion motion in the polymer matrix. The results shown by Huang *et al.* [25], Kadir *et al.* [14], Masoud *et al.* [24] and Bhide & Hariharan [27] suggest that the material with low activation energy will be a good electrolyte system.

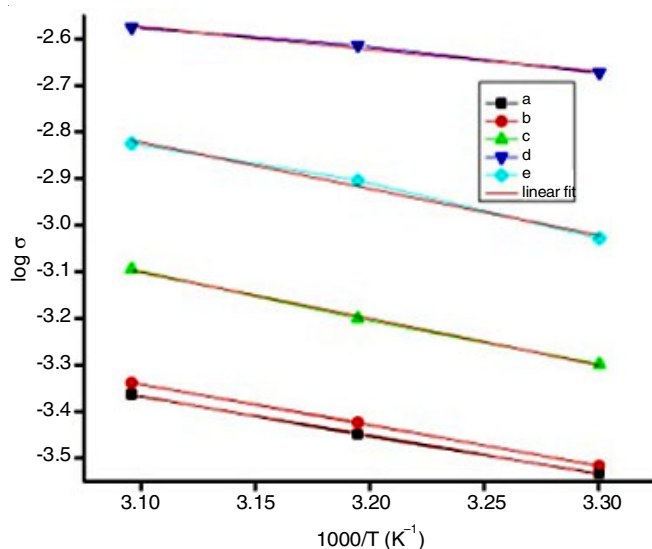


Fig. 8. $\log \sigma$ versus $1000/T$ in the temperature region of 30-50 °C for PVA-CA-AT-x nano-Al₂O₃ composite polymer electrolytes (a) x = 0, (b) 0.06, (c) 0.08, (d) 0.1 and (e) 0.3 mol

Fig. 9 shows the relationship between $\log \sigma$ and $\log f$ for 0.1 mol Al₂O₃ content of composite electrolyte at a frequency range of 10 Hz to 5 MHz and at a temperature range between 303 and 343 K. It shows that the conductivity increases with each frequency and temperature and the conductivity values are closer to that of the values obtained from Z' vs. Z'' plots. The increase in conductivity with frequency may be due to the change in mobility of the charge carriers [24], it can also be suggested that more structural relaxations with the rise of temperature causes increase in mobility of ions, thus increasing the conductivity of the composite electrolyte.

Dielectric relaxation studies: The real part (dielectric constant – ϵ') and imaginary part (dielectric loss – ϵ'') of dielectric permittivity with log frequency plots for all nano-

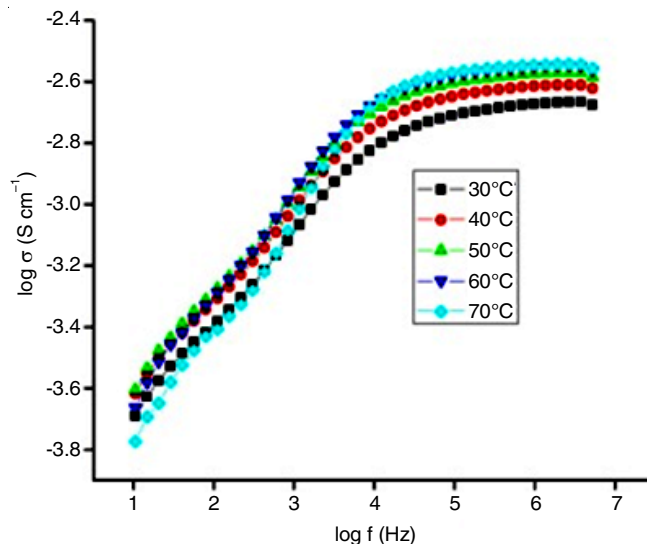


Fig. 9. $\log \sigma$ versus $\log f$ for 0.1 mol Al₂O₃ content of composite electrolyte at a frequency range of 10 Hz to 5 MHz and at a temperature range between 30 and 70 °C

alumina-free and incorporated polymer electrolytes are shown in Figs. 10 and 11, respectively. The measure of dielectric constant suggests the amount of mobile ions stored in the electrolyte system and it is observed from Fig. 10 that the value of dielectric constant at low frequency is high and decreases with increase in frequency. It can be attributed with the accumulation of free charges at the interface between electrolyte and electrodes, which contributes to large values of ϵ' . The dielectric constant obtained in our system at room temperature is high (7.21×10^7) compared with the values reported for the nano composite materials (2.2×10^6) reported by Masoud *et al.* [24]. The dielectric constant and dielectric loss values are high for 0.1 mol nano-Al₂O₃ content polymer composites when compared to that of alumina-free polymer electrolyte and this may be related to the higher conductivity values obtained for these electrolytes from the impedance analysis. This can be attributed to the presence of nano alumina in the polymer matrix and their Lewis acid-base type of interaction on the surface of nano alumina.

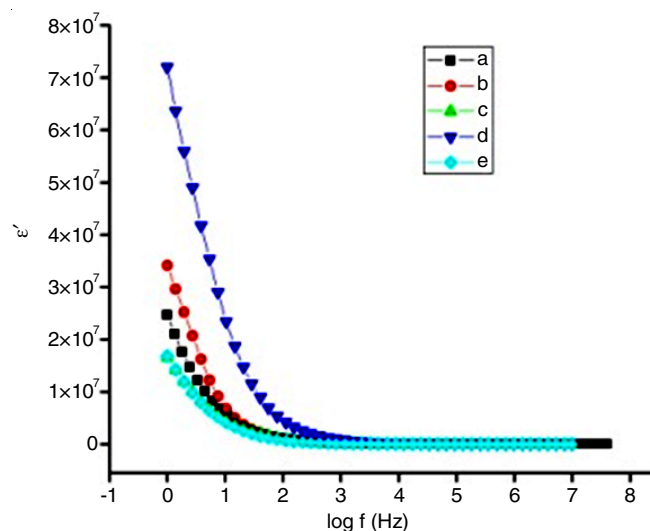


Fig. 10. Real part (ϵ') of dielectric permittivity with log frequency plots for all PVA-CA-AT-x nano-Al₂O₃ composite polymer electrolytes (a) x = 0, (b) 0.06, (c) 0.08, (d) 0.1 and (e) 0.3 mol

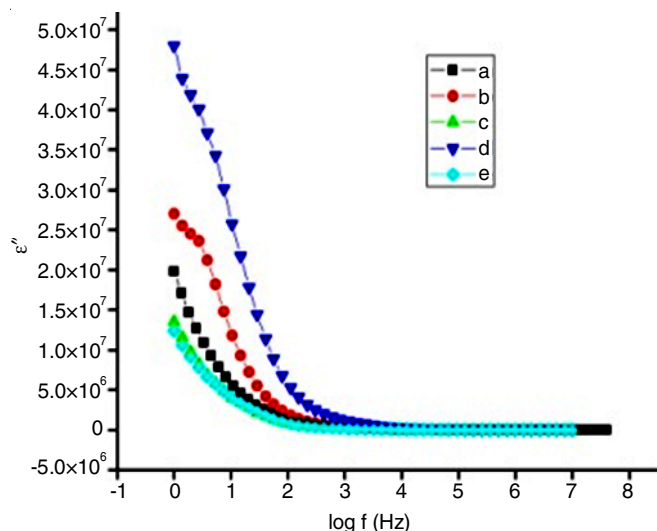


Fig. 11. Imaginary part (ϵ'') of dielectric permittivity with log frequency plots for all PVA-CA-AT-x nano- Al_2O_3 composite polymer electrolytes (a) $x = 0$, (b) 0.06, (c) 0.08, (d) 0.1 and (e) 0.3 mol

The values of dielectric constant and dielectric loss decrease for higher concentration of alumina (0.3 mol), which suggests decrease in their conductivity that may be attributed to the aggregation of nano particles in the polymer matrix which decreases the mobility of ions in the composite electrolyte.

The decrease in the dielectric constant values at the higher frequency region for all the composite electrolytes may be due to the inability of dipoles to rotate with the high frequency of the applied field.

Loss tangent spectra: Fig. 12 depicts loss tangent curves ($\tan \delta$ versus log frequency values) for PVA-CA-AT-x nano Al_2O_3 ($x = 0, 0.06, 0.08, 0.1$ and 0.3) composite polymer electrolytes. Ratio between the dielectric loss (ϵ'') and the dielectric constant (ϵ') is known as $\tan \delta$ or dissipation factor, which describes the electric energy loss of polymer electrolyte system at relaxation frequency. The frequency- dependent loss tangent curve shows an increase in $\tan \delta$ value with increasing frequency; and after attaining a maximum value at f_m , it further reduces with increase in frequency. This illustrates that relaxation of dipoles occurred in all the prepared samples [28]. From Fig. 12, the peaks for nano alumina added polymer composite electrolytes are observed to shift in the higher frequency region and it illustrates the reduction of relaxation time, which in turn increases the mobility of the cations in the polymer electrolyte. The relaxation time is calculated from the maximum frequency at which the peak is observed by using the relation $2\pi f_m \tau = 1$ and the values are listed in Table-1. From these values, the low relaxation value (2.24×10^{-7} s) is observed for the higher conducting electrolyte, which suggests that quick segmental motion occurred in the polymer chain [28]. From Fig. 6, the decrease in relaxation time with increase in nano alumina up to 0.1 mol Al_2O_3 content of polymer composite electrolyte suggests the increase in the amorphous region, which in turn enhances the ion transport by increasing the conductivity value [29]. These results are comparable with the impedance analysis values and XRD results. The incorporation of nano-sized alumina particles in the polymer matrix has been depicted in **Scheme-I** as suggested by the above studies.

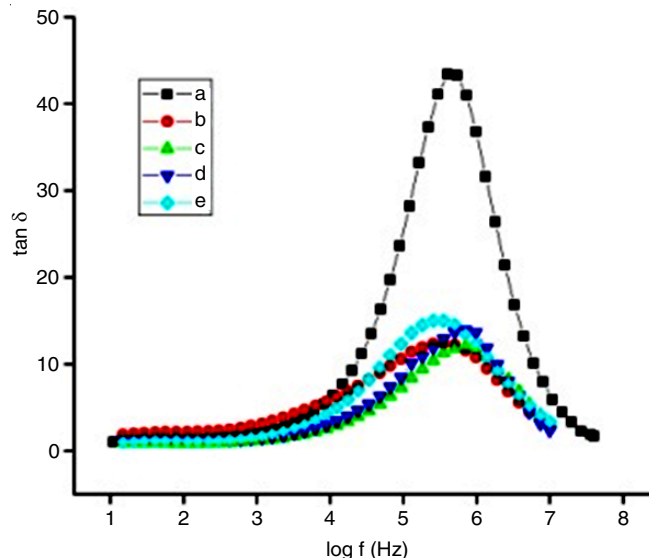


Fig. 12. Loss tangent curves for PVA-CA-AT-x nano- Al_2O_3 composite polymer electrolytes (a) $x = 0$, (b) 0.06, (c) 0.08, (d) 0.1 and (e) 0.3 mol

Battery characterization: The type of charge transport in the electrolyte can be identified with the help of transference number [29]. Various methods have already been used by many researchers. In present study, the potentiostatic polarization method was used, which is an ideal method for solid polymer electrolyte [25].

Fig. 13 showed the result of polarization measurement on PVA-CA-AT-0.1 mol nano Al_2O_3 electrolyte using stainless steel plates as blocking electrodes at DC bias voltage (1.0 V) at room temperature. The ionic transference numbers were calculated from the initial current and the final current values using the following equation:

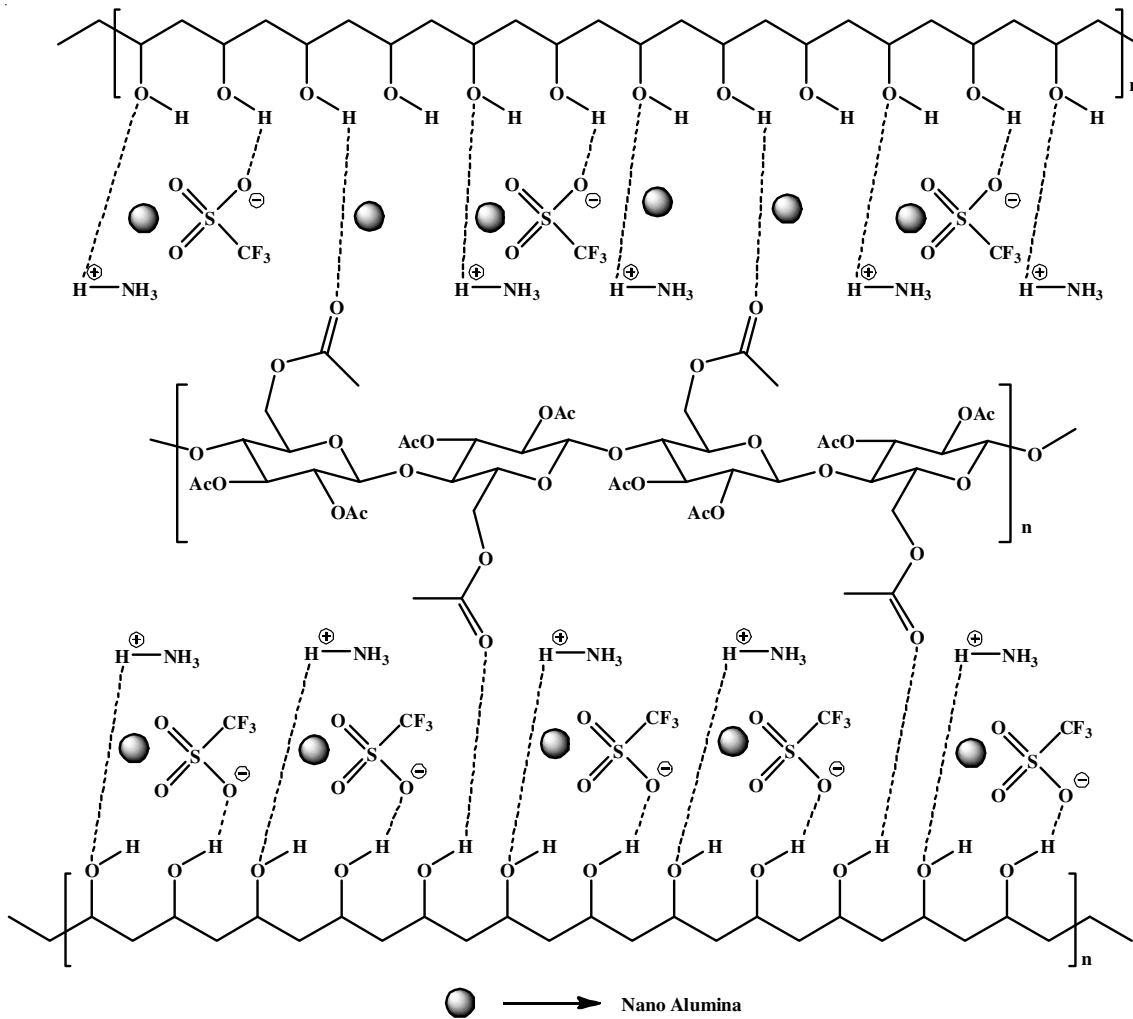
$$t_{\text{ion}} = \frac{(I_i - I_f)}{I_i} \quad (2)$$

where I_i is the initial current and I_f is the final residual current. The ionic transference number (t_{ion}) for PVA-CA-AT-0.1 nano Al_2O_3 was calculated as 0.9684, which could infer that the charge transport in the electrolyte membrane was due to the ions [8].

Fig. 14 represents the voltage with time plot for the proton battery of configuration $\text{Zn} + \text{ZnSO}_4 \cdot \text{H}_2\text{O} | \text{PVA-CA-AT-0.1 mol } \text{Al}_2\text{O}_3 | \text{PbO}_2 + \text{V}_2\text{O}_5$. The method of construction of battery is given elsewhere [8]. The open circuit voltage was measured for the above fabricated battery for a period of 17 h. The OCV was measured as 1.49 V at the beginning and it slowly decreased to 1.39 V and it was almost stable in that value for a long period [30,31]. These values are comparable with the values reported by Mishra *et al.* [32] (OCV = 1.45 V). The initial drop in OCV can be due to the polarization of the cell which arises from the concentration gradient of the reactants at the electrode surface. From this, we can attribute that the fabricated proton battery is considerably stable in the open cell condition.

Conclusion

In this paper, the polymer composite membranes were prepared by solution casting method. The ionic conductivity at the temperature range 303-343 K for PVA-CA-AT - x nano



Scheme-I: Interaction of nano alumina particles in the polymer matrix

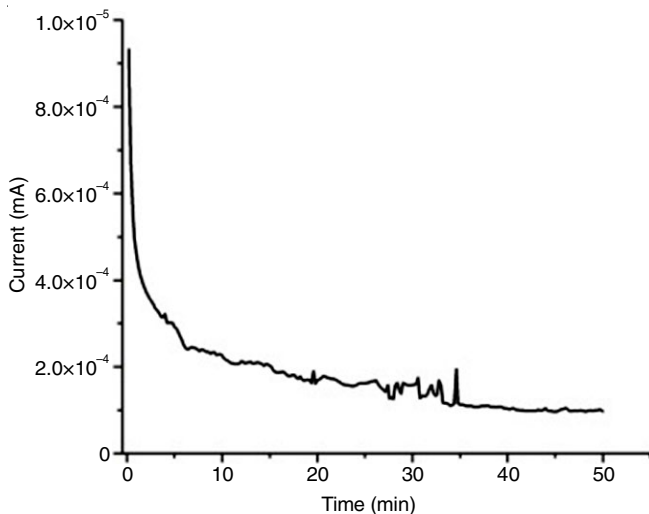


Fig. 13. Polarization curve for PVA-CA-AT-0.1 mol nano Al₂O₃ electrolyte

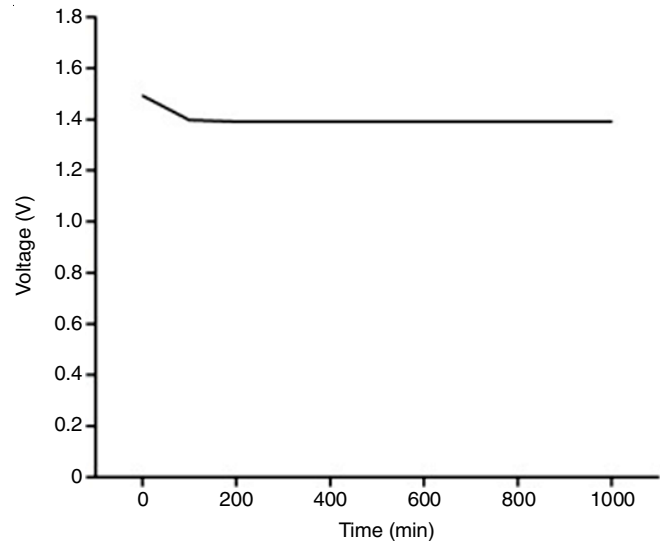


Fig. 14. Voltage versus time plot for the proton battery of configuration Zn + ZnSO₄·H₂O/PVA-CA-AT-0.1 mol wt % Al₂O₃| PbO₂+V₂O₅

Al₂O₃ ($x = 0, 0.06, 0.08, 0.1$ and 0.3 mol) composite polymer electrolytes were measured by AC impedance spectroscopy analysis. All the membranes were characterized by infrared spectra, X-ray diffraction and DSC analysis. The change in intensity and shifts of IR peaks confirm the complexation between the salt and polymer matrix. It also confirms the presence of nano filler in the composite polymer electrolyte

without chemically bonded to the polymer matrix. X-ray diffraction results confirm the increased amorphous nature of the composite electrolyte, which in turn increases conductivity value upon the addition of filler. DSC analyses revealed the melting points of all the membranes. The electrolyte containing

0.1 mol content of nano alumina showed the highest conductivity value of 2.03×10^{-3} S/cm at room temperature. The dielectric constant and dielectric loss values of 7.21×10^7 and 4.79×10^7 at room temperature, respectively, were measured by AC impedance spectroscopy studies. The transference number for this composite electrolyte confirms the ionic mobility in the electrolyte. The measured OCV for the sustained period of 17 h confirms its stability as a suitable electrolyte for an electrochemical cell. The high values of ionic conductivity, dielectric constant and dielectric loss of the polymer composite electrolyte lead to encourage the addition of filler in the polymer matrix and make this composite electrolyte membrane a promising material in devices using the solid polymer electrolyte.

ACKNOWLEDGEMENTS

The authors thank Department of Physics and SAIF, IIT Madras, Chennai, India for providing the characterization facilities.

CONFLICT OF INTEREST

The authors declare that there is no conflict of interests regarding the publication of this article.

REFERENCES

- J. Qiao, J. Fu, R. Lin, J. Ma and J. Liu, *Polymer*, **51**, 4850 (2010); <https://doi.org/10.1016/j.polymer.2010.08.018>.
- N.N.B. Ramly, The Preparation and Characterization of Sulfonated Poly (Ether Ether Ketone) and Cellulose Acetate (SPEEK-CA) Membrane in Proton Exchange Membrane Fuel Cells (PEMFCs) By UV-Crosslink Technique, Humanities, Science and Engineering (CHUSER)-2012 IEEE Colloquium on, IEEE: pp. 637-641 (2012).
- J. Qiao, T. Hamaya and T. Okada, *Polymer*, **46**, 10809 (2005); <https://doi.org/10.1016/j.polymer.2005.09.007>.
- X. Li, Y. Wu, K. Hua, S. Li, D. Fang, Z. Luo, R. Bao, X. Fan and J. Yi, *Colloid Polym. Sci.*, **296**, 1395 (2018); <https://doi.org/10.1007/s00396-018-4351-6>.
- S. Gurulakshmi, S. Madheswaran, S. Karthikeyan, S. Selvasekarapandian and S. Monisha, ed.: J. Ebenezer, Study of PVA/CA/NH₄SCN/Ethylene Carbonate/Al₂O₃ Polymer Nano-Composite Electrolyte System, In: Recent Trends in Materials Science and Applications, Springer Proceedings in Physics, Springer: Cham, vol. 189, pp. 263-275 (2017).
- S. Rajendran, M. Sivakumar and R. Subadevi, *Solid State Ion.*, **167**, 335 (2004); <https://doi.org/10.1016/j.ssi.2004.01.020>.
- M. Dissanayake, L. Bandara, L. Karaliyadda, P. Jayathilaka and R. Bokalawala, *Solid State Ion.*, **177**, 343 (2006); <https://doi.org/10.1016/j.ssi.2005.10.031>.
- N.K. Anuar, N. Zainal, M. Nor Sabirin and R.H.Y. Subban, In Studies of poly (ethyl methacrylate) complexed with ammonium trifluoromethane Sulfonate, Advanced Materials Research, Trans. Tech. Publ., pp 19-23 (2012).
- S. Klongkan and J. Pumchusak, *Electrochim. Acta*, **161**, 171 (2015); <https://doi.org/10.1016/j.electacta.2015.02.074>.
- B. Liang, S. Tang, Q. Jiang, C. Chen, X. Chen, S. Li and X. Yan, *Electrochim. Acta*, **169**, 334 (2015); <https://doi.org/10.1016/j.electacta.2015.04.039>.
- D.S. Kim, H.B. Park, J.W. Rhim and Y.M. Lee, *J. Membr. Sci.*, **240**, 37 (2004); <https://doi.org/10.1016/j.memsci.2004.04.010>.
- R. Hodge, G.H. Edward and G.P. Simon, *Polymer*, **37**, 1371 (1996); [https://doi.org/10.1016/0032-3861\(96\)81134-7](https://doi.org/10.1016/0032-3861(96)81134-7).
- C.-P. Liu, C.-A. Dai, C.-Y. Chao and S.-J. Chang, *J. Power Sources*, **249**, 285 (2014); <https://doi.org/10.1016/j.jpowsour.2013.10.117>.
- M. Kadir, S. Majid and A. Arof, *Electrochim. Acta*, **55**, 1475 (2010); <https://doi.org/10.1016/j.electacta.2009.05.011>.
- S. Chintapalli, C. Zea and R. Frech, *Solid State Ion.*, **92**, 205 (1996); [https://doi.org/10.1016/S0167-2738\(96\)00473-0](https://doi.org/10.1016/S0167-2738(96)00473-0).
- C.V. Rohatgi, N.K. Dutta and N.R. Choudhury, *Nanomaterials*, **5**, 398 (2015); <https://doi.org/10.3390/nano5020398>.
- S. Ramesh, R. Shanti and E. Morris, *Carbohydr. Polym.*, **91**, 14 (2013); <https://doi.org/10.1016/j.carbpol.2012.07.061>.
- R. Kumar, J.P. Sharma and S. Sekhon, *Eur. Polym. J.*, **41**, 2718 (2005); <https://doi.org/10.1016/j.eurpolymj.2005.05.010>.
- M.R. Johan, O.H. Shy, S. Ibrahim, S.M. Mohd Yassin and T.Y. Hui, *Solid State Ion.*, **196**, 41 (2011); <https://doi.org/10.1016/j.ssi.2011.06.001>.
- L. Agrawal and A. Awadhia, *Bull. Mater. Sci.*, **27**, 523 (2004); <https://doi.org/10.1007/BF02707280>.
- S. Rudhzhiah, N. Mohamed and A. Ahmad, *Int. J. Electrochem. Sci.*, **8**, 421 (2013).
- A. Mohamad, N. Mohamed, Y. Alias and A. Arof, *J. Alloys Compd.*, **337**, 208 (2002); [https://doi.org/10.1016/S0925-8388\(01\)01916-8](https://doi.org/10.1016/S0925-8388(01)01916-8).
- S. Patel, R. Patel, A. Awadhia, N. Chand and S. Agrawal, *Pramana*, **69**, 467 (2007); <https://doi.org/10.1007/s12043-007-0148-8>.
- E.M. Masoud, A.-A. El-Bellihi, W. Bayoumy and M. Mousa, *J. Alloys Compd.*, **575**, 223 (2013); <https://doi.org/10.1016/j.jallcom.2013.04.054>.
- X. Huang, X. Ma, R. Wang, L. Zhang and Z. Deng, *Solid State Ion.*, **267**, 54 (2014); <https://doi.org/10.1016/j.ssi.2014.08.012>.
- D. Praveen, S. Bhat and R. Damle, *Ionics*, **17**, 21 (2011); <https://doi.org/10.1007/s11581-010-0476-4>.
- A. Bhide and K. Hariharan, *Eur. Polym. J.*, **43**, 4253 (2007); <https://doi.org/10.1016/j.eurpolymj.2007.07.038>.
- C. Bhatt, R. Swaroop, A. Arya and A. Sharma, *J. Mater. Sci. Eng. B*, **5**, 418 (2015).
- M.L. Verma and H.D. Sahu, *Ionics*, **23**, 2339 (2017); <https://doi.org/10.1007/s11581-017-2063-4>.
- A.J. Bhattacharyya and J. Maier, *Adv. Mater.*, **16**, 811 (2004); <https://doi.org/10.1002/adma.200306210>.
- S.B. Aziz, R.M. Abdullah, M.A. Rasheed and H.M. Ahmed, *Polymers*, **9**, 338 (2017); <https://doi.org/10.3390/polym9080338>.
- K. Mishra, S.A. Hashmi and D.K. Rai, *High Perform. Polym.*, **26**, 672 (2014); <https://doi.org/10.1177/09544008314537540>.